Quaternary Science Reviews 332 (2024) 108636

Contents lists available at ScienceDirect

Quaternary Science Reviews

journal homepage: www.elsevier.com/locate/quascirev

The impact of elevated nutrients on the Holocene evolution of the Great Barrier Reef

Kelsey L. Sanborn [a], Jody M. Webster [a,*], Dirk Erler [b], Gregory E. Webb [c], Marcos Salas-Saavedra [c,d], Yusuke Yokoyama [e]

[a] Geocoastal Research Group, School of Geosciences, University of Sydney, NSW, 2006, Australia
[b] Centre for Coastal Biogeochemistry, Faculty of Science and Engineering, Southern Cross University, Lismore, NSW, 2480, Australia
[c] School of Environment, The University of Queensland, QLD, 4072, Australia
[d] Department of Geosciences, Princeton University, Princeton, USA
[e] Atmosphere and Ocean Research Institute, Department of Earth and Planetary Sciences, University of Tokyo, Chiba, Japan

ARTICLE INFO

Handling editor: I Hendy

Keywords:
Coral
Geochemical proxies
Nutrients
Water quality
Sea-level change
Holocene
Great barrier reef

ABSTRACT

The initiation of the Holocene Great Barrier Reef coincided with rapid environmental change as sea level rose and inundated the shelf. Core data from One Tree Reef (southern Great Barrier Reef) shows coral growth started by ~8.2 ka, but accretion between 8 and 7 ka was slower, occurred in deeper water, and comprised more sediment-tolerant coral communities compared to growth following sea-level stabilization. It has been postulated that environmental stressors (e.g. increased turbidity and nutrients) suppressed and delayed reef growth, however direct data supporting this hypothesis are scarce. Here we combine the isotopic composition of skeletal bound organic nitrogen ($\delta^{15}N$) and Ba/Ca ratios of coral skeletons with published geochemical proxies of terrestrial sediment discharge to constrain Holocene water conditions at One Tree Reef. Between 8 and 7 ka the skeletal $\delta^{15}N$ values from multiple corals and genera were elevated (average of 8.45 ± 0.89‰) relative to the early transgression and following sea-level stabilization (average of 7.04 ± 0.82‰). We propose that elevated $\delta^{15}N$ in corals reflects the discharge of deep terrestrial soil nitrogen resulting from high runoff. This is supported by Ba/Ca measurements and published rare earth element and yttrium (REE + Y) geochemical proxies in coral and reefal microbialites from the same cores. These data suggest that increased terrigenous discharge of sediment and nutrients did not inhibit reef growth, rather led to the establishment of slower-growing, deeper and more sediment-tolerant coral communities. Understanding the capacity for reef growth under adverse environmental conditions provides insight into thresholds and resilience of the GBR over centennial-millennial timescales.

1. Introduction

The early Holocene initiation of the Great Barrier Reef (GBR) is an important case study to investigate the ability of coral reef systems to grow and withstand rapid environmental changes (Marshall and Davies, 1982; Dechnik et al., 2015; Sanborn et al., 2020). This time interval was marked by rapid relative sea-level (RSL) rise (~6–7 m/ka; Sloss et al., 2007; Lewis et al., 2013), increasing sea surface temperatures (SST) (+4° mean annual water temperature anomaly between 8 and 6 ka; Gagan et al., 2004; Sadler et al., 2016; Leonard et al., 2018), a wetter climate contributing to increased terrestrial runoff (Hembrow et al., 2014), along with the reworking of terrestrial shelf sediments during the transgression of the GBR shelf (Davies and Kinesy, 1977; Hallock and Schlager, 1986). These factors are generally recognized as being detrimental to reef growth, particularly for present reef systems threatened by rising SSTs, declining water quality, and increased nutrient runoff (Hughes et al., 2003; Pandolfi et al., 2003; Brodie et al., 2012; Waterhouse et al., 2017). Despite these unfavorable environmental conditions, studies across the GBR show extensive early Holocene reef growth by ~8 ka, following a lag of ~1200–700 years between the flooding of the shelf and first coral growth (Dechnik et al., 2015; Sanborn et al., 2020). Previous work from One Tree Reef (OTR) (Fig. 1), southern GBR, showed that while the composition of early reef-building communities prior to 7 ka was primarily indicative of deeper or more turbid water settings, there is also evidence for clear-water communities from the initial coral growth 8.22 ± 0.05 ka (Dechnik et al., 2015; Sanborn et al.,

* Corresponding author.
E-mail address: jody.webster@sydney.edu.au (J.M. Webster).

https://doi.org/10.1016/j.quascirev.2024.108636
Received 10 December 2023; Received in revised form 22 March 2024; Accepted 22 March 2024
Available online 25 April 2024

2020).

Coral skeletal isotope geochemistry can provide useful proxies to investigate environmental controls on early Holocene reef development, including SST, salinity and phosphorous concentration (Alibert and McCulloch, 1997; Druffel, 1997; Montagna et al., 2006; Sadler et al., 2016). Nitrogen (N) isotope signatures ($\delta^{15}N$, where $\delta^{15}N = [(^{15}N/^{14}N)_{sample}/(^{15}N/^{14}N)_{air}] - 1$) in organic material bound within coral skeletons have been used to trace sources and availability of oceanic N in both modern and fossil corals, and has similarly been applied to red and green calcareous algae (Marion et al., 2005; Wang et al., 2017; Erler et al., 2019; McNeil et al., 2021). These studies rely on the underlying premise that relative changes in $\delta^{15}N$ in a coral skeleton reflect shifts in the isotopic composition of N in the environment, which then is preserved in trace organic compounds in skeletal aragonite (Studer et al., 2018; Erler et al., 2019). While a species-specific offset between coral skeletal organic and coral tissue $\delta^{15}N$ occurs, the skeletal material robustly reflects the $\delta^{15}N$ of the coral tissue, which in turn reflects the $\delta^{15}N$ of the water column (Erler et al., 2015; Wang et al., 2016). Paired with radiometric dates, changes in $\delta^{15}N$ values over time can represent increased inputs of terrigenous N, N_2 fixation, or stronger upwelling, and thus provide a valuable proxy for N input and cycling (Erler et al., 2015, 2019; Wang et al., 2015; Duprey et al., 2019). This has additionally been applied to studies of terrestrial runoff on the modern GBR, where highly enriched $\delta^{15}N$ values (12–14‰) tracked increased river discharge during extreme flood events (Jupiter et al., 2008). Ba/Ca ratios in coral cores provide additional records of suspended sediment loads, and thus nutrients, with positive anomalies in skeletal Ba/Ca ratios correlating with major river discharge events in the GBR (McCulloch et al., 2003; Saha et al., 2016), although Ba also may be affected by other biogeochemical cycling (Sinclair, 2005; Lewis et al., 2018; Saha et al., 2018b).

While nutrient availability is widely accepted as a control on the modern spatial distribution and growth capacity of coral reefs, it is also possible that elevated nutrient concentrations from increased upwelling, or terrestrial discharge, played a role in suppressing coral calcification during the early Holocene (Kinsey and Davies, 1979; Macintyre, 1988). Although there has not been adequate geochemical data to test this claim, it has been widely postulated that coral reefs were negatively impacted by increased nutrient availability in the early Holocene, causing lags and turn offs of reef growth in the Caribbean and elsewhere (Hallock and Schlager, 1986). In order to investigate the relationship between reef growth and coral skeletal $\delta^{15}N$, we used Holocene corals from OTR, which is one of the most widely studied reefs on the GBR from a geologic standpoint (Davies and Kinesy, 1977; Marshall and Davies, 1982). Previous work on OTR has provided high-resolution geochronology and analyses of centennial-scale shifts in reef-building communities over the Holocene (Sanborn et al., 2020). In this study, we present the first record of coral $\delta^{15}N$ and Ba/Ca from well dated Holocene reef

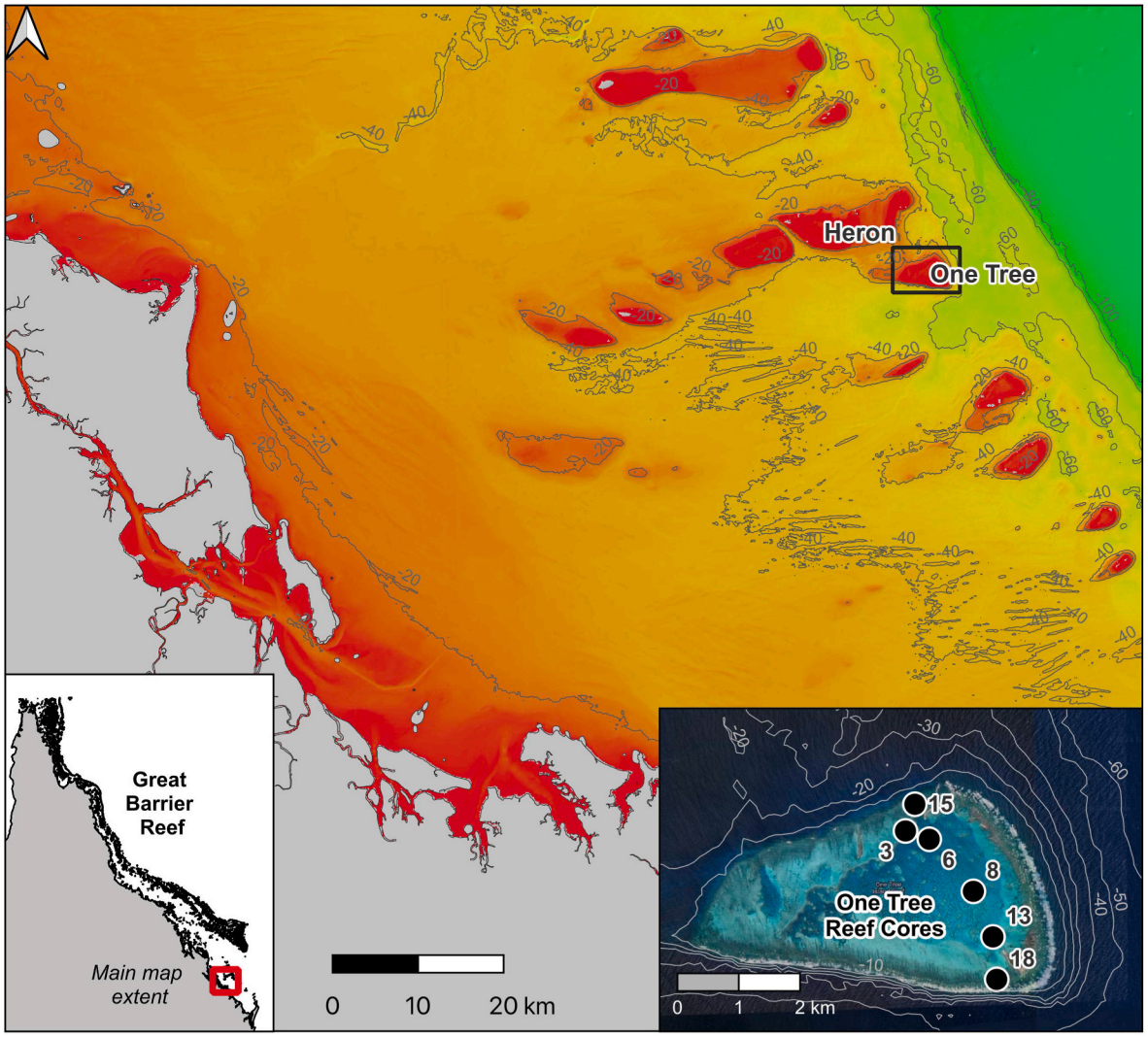

Fig. 1. Location of One Tree and Heron Reefs, and location of One Tree Reef Holocene cores (inset) (bathymetry source (Beaman, 2010)).

cores in order to characterize nutrient conditions during the early Holocene development of the southern GBR over centennial-millennial timescales. This demonstrates how the GBR has grown under typically adverse conditions in the past and has implications for predicting the growth of the GBR under future environmental change.

2. Methods

2.1. Coral isotopic and trace element analyses

A 2015 drilling campaign yielded 12 new reef cores across different OTR settings, from which detailed assessments of Holocene reef communities and geochronology have been reported (Sanborn et al., 2020). Previously dated *Porites*, *Isopora*, and *Acropora* coral samples (n = 18) from these cores were selected for isotopic analysis, screened for diagenesis using thin section petrography, X-Ray Diffraction (XRD), and Scanning Electron Microscope (SEM) and imaged using computed tomography (CT) to identify annual growth bands. Four additional corals were selected from a prior OTR drilling campaign (Dechnik et al., 2015). Two samples were collected from each selected coral colony. At least one high and one low density band were sampled from each coral where possible to identify, so as to avoid seasonal differences in terrestrial flux (e.g., Saha et al., 2018a, 2019). Powders of the corymbose branching *Acropora* colonies were drilled from the inter-branch skeleton (consisting of both coenosteum and corallites), which has similar annual density banding to massive *Porites* and good potential for use in paleoclimate reconstructions (Sadler et al., 2014, 2015). Corals were sampled using a Dremel tool and homogenized into a 100 mg sample (Supplementary Fig. 1) using an agate mortar and pestle before chemical cleaning (Wang et al., 2015). Due to potential differences in trophic levels between coral genera, we did not make direct comparisons between coral data, only the cumulative dataset.

Homogenized and cleaned powders were dissolved in HCl, after which organic N was oxidized to NO_3^-, converted to N_2O, and then analyzed for $\delta^{15}N$ following Wang et al. (2015). Nitrogen isotopes were measured at Southern Cross University using a Thermo Delta V Plus Isotope Ratio Mass Spectrometer coupled to a Thermo GasBench II interface system to concentrate the nitrous oxide following Erler et al. (2019). Each of the two multi-band homogenized samples per coral were run separately in triplicate with an analytical precision of 0.5 ‰. Means of the values of the two sets of triplicates per coral colony were analyzed in order to present multi-year averages and avoid seasonal variation, as there are high seasonal differences in discharge and thus transport of terrigenous material to the GBR (e.g., Saha et al., 2018a, 2019). Ba/Ca concentrations were measured at the Atmosphere and Ocean Research Institute of the University of Tokyo using inductively coupled plasma-atomic emission spectrometry (iCAP6300 Duo, Thermo Fisher Scientific) including XSTC-13 (multi-element standard solution, SPEX) and JCp-1 (a coral standard material, Okai et al., 2002).

2.2. Incorporated coral geochronology and geochemical proxy data

Eighteen of the coral samples had been previously dated directly (i.e., the reported age is from the same coral colony), and an age estimate for three additional undated coral samples were extrapolated from a closely adjacent dated sample (see Table 1). This represents an additional conservative age error of 60 years (in addition to the 2σ age uncertainty) based on mean vertical accretion rates (Sanborn et al., 2020). For comparison to other valuable geochemical proxies for water quality, rare earth element and yttrium (REE + Y) data from corals and microbialites (Salas-Saavedra, 2019; Salas-Saavedra et al., 2022) from the same OTR reef cores, in combination with measurements from the nearby (~7 km away) Heron Reef, were included.

3. Results

A distinct peak in skeletal $\delta^{15}N$ of *Porites* and acroporids from OTR is evident between 8 and 7 ka (Fig. 2A; Table 1). This enhancement is clearly demonstrated in the patch reef and windward margin samples, with the highest value of 9.57 ± 0.37‰ measured in a patch reef *Porites* with an age of 7.60 ± 0.03 ka. The leeward margin samples have a peak value of 8.36 ± 0.44‰ slightly later at 6.78 ± 0.06 ka.

This is consistent with trends and values of the measurements between the different coral genera (*Porites, Acropora* and *Isopora*). Comparisons between time bins (Fig. 2B) show: (1) 7.04 ± 0.82‰ average value for all samples younger than 7 ka (n = 11), (2) 8.45 ± 0.89‰ average value for all samples between 8 and 7 ka (n = 8), and (3) and 6.93 ± 0.32‰ average value for samples older than 8 ka (n = 3). A One

Table 1
Averaged $\delta^{15}N$ and Ba/Ca OTR coral results with paired age data.

Sample	Reef setting	Coral genus	Averaged $\delta^{15}N$ ‰ (1σ error)[a]	Ba/Ca μmol/mol (1σ error)	Age ka BP (2σ error)	Source for age[b]
OTI_Modern	Patch reef	*Porites*	6.88 (0.23)		0	N/A
OTI_3_8_D	Leeward	*Acropora*	6.38 (0.44)		1.73 (0.42) [c]	2
OTI_8_2_2	Patch reef	*Porites*	5.82 (0.25)	11.9 (0.02)	3.40 (0.01)	1
OTI_18_2_2	Windward	*Acropora*	7.34 (0.56)	19.3 (0.04)	6.04 (0.02)	1
OTI_8_7_2	Patch reef	*Porites*	5.71 (0.38)	13.3 (0.03)	6.22 (0.02)	1
OTI_8_7_2_R2	Patch reef	*Porites*	7.69 (0.22)		6.22 (0.02)	1
OTI_13_1_4	Patch reef	*Acropora*	7.13 (0.34)	5.99 (0.01)	6.23 (0.01)	1
OTI_13_2_3	Patch reef	*Isopora*	7.47 (0.61)		6.34 (0.02)	1
OTI_6_5_B	Patch Reef	*Porites*	6.97 (0.68)	2.17 (0.01)	6.43 (0.87)	2
OTI_15_1_3	Leeward	*Acropora*	8.36 (0.44)		6.78 (0.06)	1
OTI_15_3_2	Leeward	*Acropora*	7.72 (0.37)		6.98 (0.03)	1
OTI_13_5_2	Patch reef	*Acropora*	7.55 (0.37)		7.21 (0.02)	1
OTI_18_5_4	Windward	*Acropora*	9.03 (0.84)	5.59 (0.01)	7.31 (0.03)	1
OTI_13_6_4	Patch reef	*Acropora*	7.73 (0.58)		7.39 (0.02)	1
OTI_8_8_3	Patch reef	*Porites*	9.57 (0.37)	5.61 (0.01)	7.60 (0.03)	1
OTI_18_7_3	Windward	*Acropora*	8.98 (0.39)	7.72 (0.01)	7.73 (0.09)	1
OTI_15_6_2	Leeward	*Acropora*	7.07 (0.19)		7.90 (0.04)	1
OTI_13_7_2	Patch Reef	*Acropora*	8.53 (0.47)	7.79 (0.01)	7.91 (0.03)	1
OTI_6_10_B	Patch Reef	*Porites*	9.14 (0.48)	8.24 (0.01)	7.95 (0.80) [c]	2
OTI_6_10_E	Patch Reef	*Porites*	7.29 (0.34)	3.14 (0.01)	8.15 (0.17) [c]	3
OTI_13_8_2	Patch reef	*Isopora*	6.84 (0.51)	6.16 (0.01)	8.17 (0.02)	1
OTI_15_7_3	Leeward	*Acropora*	6.65 (0.34)		8.22 (0.05)	1

[a] Average of two sets of triplicate sample measurements.
[b] (1) Sanborn et al. (2020); (2) Davies and Hopley (1983); (3) Dechnik et al. (2015).
[c] Exact piece not dated; age and error from an adjacent piece is reported, and we estimate an additional conservative age error of 60 yrs based on mean vertical accretion rates (Sanborn et al., 2020).

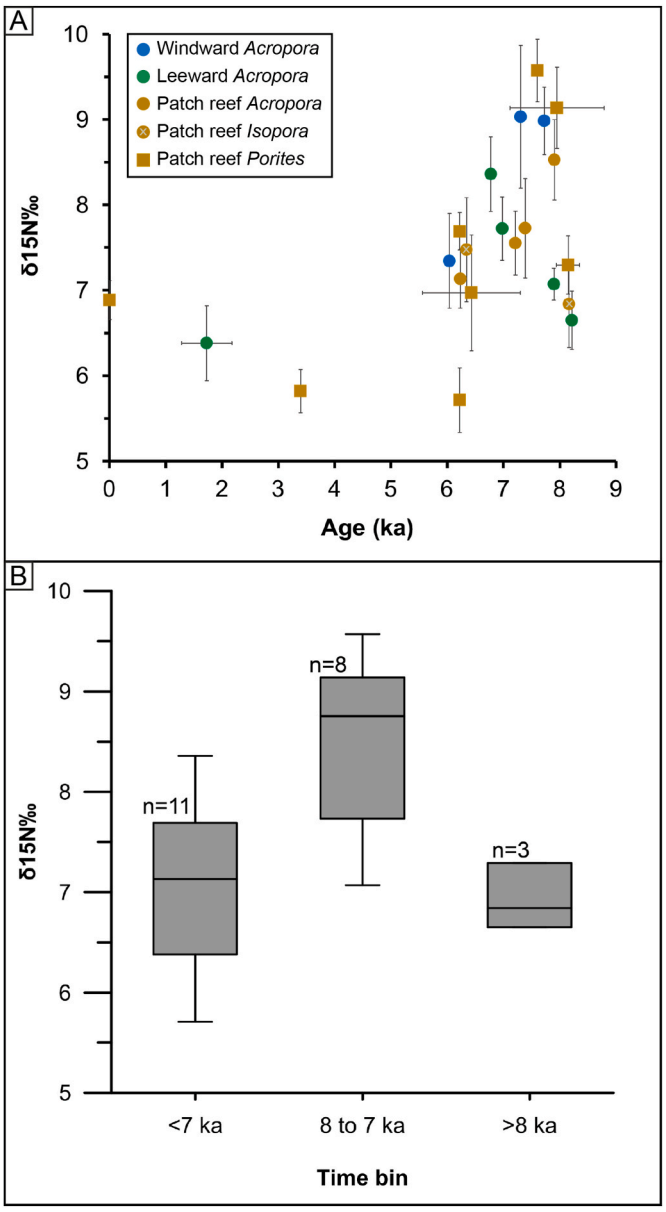

Fig. 2. (A) The $\delta^{15}N$ measurements from all OTR Holocene corals, with each point representing an average value of the six measurements per coral colony (triplicate runs of two samples) with standard deviation plotted as the vertical error. Coral samples are colored by reef setting, and genera showed by shape. Horizontal 2σ age errors are shown. (B) Box and whisker plot for the averaged $\delta^{15}N$ values for One Tree coral samples in time bins, showing the interquartile ranges (i.e., Q1, median and Q3) for each group, and the highest and lowest values indicated by the whiskers.

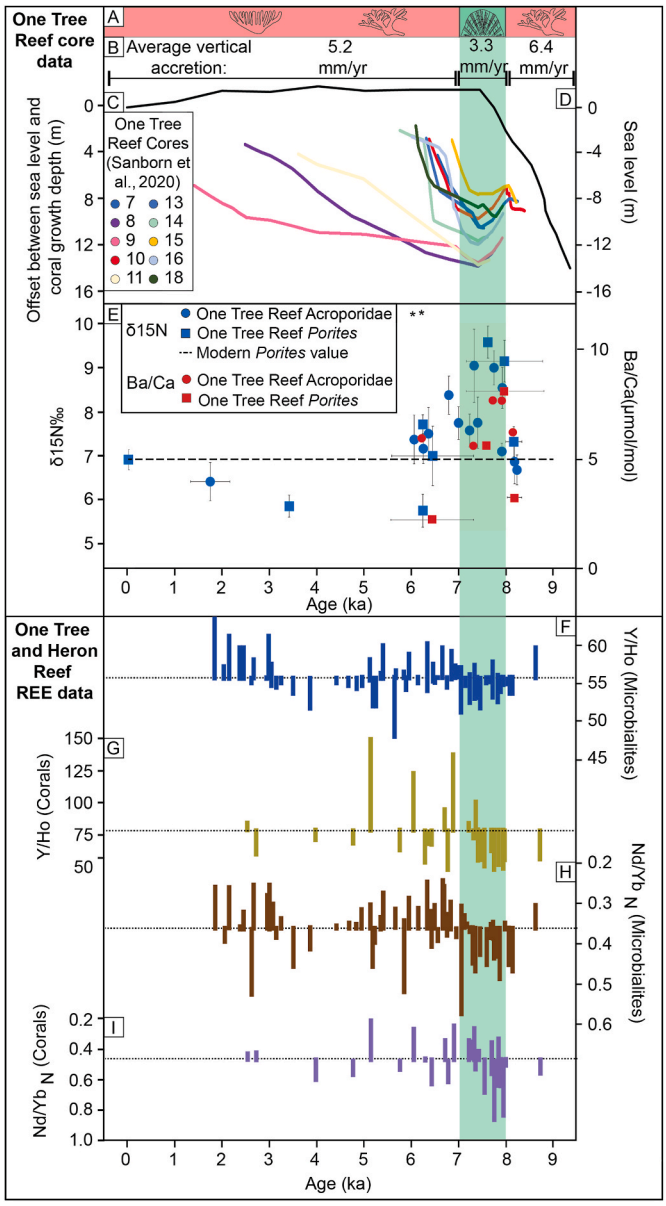

Fig. 3. Compiled datasets of Holocene reef growth and environment with the 8–7 ka time band shaded in green. (A) Dominant coral reef assemblage identified on OTR over time from Sanborn et al. (2020) with predominantly branching Acroporidae (red, branching coral symbols) <7 ka and >8 ka, and predominantly (sub)massive or encrusting Poritidae and Merulinidae (green, massive coral symbol) 8-7 ka. (B) Binned average OTR vertical accretion rates during <7 ka (5.2 mm/yr), 8–7 ka (3.3 mm/yr), and >8 ka (6.4 mm/yr) from Sanborn et al. (2020). (C) Paleowater depth represented by the offset between dated coral depth and sea level (Sanborn et al., 2020) using (D) eastern Australia sea level best estimate (Sloss et al., 2007; Lewis et al., 2013). (E) New $\delta^{15}N$ and Ba/Ca measurements from all OTR corals (average values of the triplicate runs of two samples per coral colony) with standard deviation vertical errors, plotted against age with 2σ horizontal age errors (this study). * marks measurements beyond plotted axis. Below, concentration plots of REE + Y proxies from Salas-Saavedra (2019) and Salas-Saavedra et al. (2022) from One Tree and Heron reefs with dashed lines as average value for each proxy. Y/Ho ratios from (F) microbialite and (G) coral show relatively low values in the early Holocene. Higher normalized Nd/Yb ratios (lower bars) from (H) microbialites and (I) corals indicate reduced light REE depletion until ~7.5 ka. Both signify increased influence of terrigenous mud.

Way ANOVA test shows that the 8 to 7 ka time bin average is significantly different (higher) than the average values from the other two time bins before and after (F statistic = 8; p = 0.003), while the averages of the <7 ka and >8 ka bins are indistinguishable. The highest Ba/Ca value of 19.3 ± 0.04 μmol/mol was measured in an *Acropora* with an age of 6.04 ± 0.02 ka (Fig. 3). Three Ba/Ca measurements over 10 μmol/mol were measured on corals between 3.40 ± 0.01 ka and 6.22 ± 0.02 ka. A second lower peak of 8.24 ± 0.01 μmol/mol occurs at 7.95 ± 0.80 ka.

4. Discussion

These data represent the first reconstructed centennial-millennial-scale coal record of Holocene $\delta^{15}N$ in the GBR. It shows significantly

elevated $\delta^{15}N$ values between 8 and 7 ka using OTR coral data from a variety of reef settings and multiple coral genera (Fig. 3). The $\delta^{15}N$ of coral tissue, and subsequently the $\delta^{15}N$ of N in the coral's skeletal organic matrix, can vary as a response to both the availability and source of N to the reef system. As in the modern GBR, the dominant sources of N to the Holocene reefs were likely to be N_2 fixation, upwelling, and terrestrial discharge (Erler et al., 2016, 2020; Wang et al., 2016). Nitrogen fixation lowers the $\delta^{15}N$ of the oceanic N pool and therefore can be ruled out as the driving influence on increasing skeletal $\delta^{15}N$ after the transgression. Upwelling can deliver N to shallow coral reefs with an isotope value similar to the deep ocean (~6.5‰; Yoshikawa et al., 2015); this would result in a maximum coral $\delta^{15}N$ of 8.5‰, accounting for the ~2‰ fractionation of $\delta^{15}N$ between corals and their N source (Wang et al., 2016). However coral and microbialite REE + Y data (Salas-Saavedra, 2019; Salas-Saavedra et al., 2022) from both One Tree and Heron reefs (Fig. 3F–I) shows evidence for terrestrially-influenced early Holocene water quality rather than an influence from upwelling. Compared to average Holocene values, there were reduced Y/Ho ratios until 7 ka (Fig. 3F and G) and reduced light REE depletion shown by higher normalized Nd/Yb ratios until ~7.5 ka (Fig. 3H and I). These suggest an increased influence of terrigenous mud on the regional seawater composition (Saha et al., 2016, 2019; Salas-Saavedra, 2019; Salas-Saavedra et al., 2022).

A coral record from the inner-mid-shelf region of the GBR indicates that prior to European settlement, Ba/Ca values > 6 μmol/mol record high suspended sediment caused by Burdekin River flooding (McCulloch et al., 2003). The elevated values of >7 μmol/mol between 7.73 ± 0.09 and 7.95 ± 0.80 ka support the hypothesis of increased terrigenous inputs during this time, consistent with the elevated $\delta^{15}N$ (Fig. 3E). The elevated values of >10 μmol/mol between 3.40 ± 0.01 and 6.22 ± 0.02 ka indicate high suspended sediment loads after sea level stabilized, which is not similarly reflected by elevated $\delta^{15}N$ values.

The elevated $\delta^{15}N$ values between 8 and 7 ka (Fig. 3E) also correlate with several other variations in environmental parameters and reef growth (Fig. 3). During this time, there are predominantly (sub)massive or encrusting Poritidae and Merulinidae recorded in the OTR cores, and fewer shallow branching Acroporidae, which are prevalent earlier than 8 ka and after 7 ka (Fig. 3A). The reef cores also record the slowest average vertical accretion rate (~3 mm/yr) between 8 and 7 ka, which is 2–3 mm/yr slower than earlier or later time periods up until the reefs had occupied available accommodation (Fig. 3B). Furthermore, reef growth between 8 and 7 ka occurs in deeper water (5–14 m deep), measured by the offset between the best RSL estimate (Fig. 3D) and the depth of coral growth as reported in the new OTR cores (Fig. 3C; Sanborn et al., 2020). This was also a time of rapid RSL rise (~6–7 m/ka), and once stabilized after ~7 ka (Sloss et al., 2007; Lewis et al., 2013), the reef evidently both "caught up" and "cleaned up", resulting in the more rapid (5 mm/yr) vertical accretion of shallow reef communities, which coincided with decreased $\delta^{15}N$ values. Thus, geochemical evidence from two independent proxies in coral and coral-associated microbialites support a strong terrestrial influence on the coral $\delta^{15}N$ signature between 8 and 7 ka. However, it is acknowledged that substantial muds were not visibly preserved within this core interval, which might be expected in a very turbid environment.

Terrestrial fixed N has a highly dynamic $\delta^{15}N$ range depending on its source and exposure to microbial processing. Forested soils from the GBR catchment have a $\delta^{15}N$ of 6.6 ± 0.97‰ (Bahadori et al., 2019), however microbial processing of this N can increase the $\delta^{15}N$ markedly (12‰ or greater; Marion et al., 2021). Erler et al. (2015) provided evidence that deeper soil layers, which are likely to have higher $\delta^{15}N$ (Hobbie and Ouimette, 2009), were being discharged to the modern coastal GBR, with values of up to 9.5‰ in terrestrial humic material recovered from coral skeleton in the inshore GBR (Magnetic Island). We propose that the increase in $\delta^{15}N$ from 8 ka to 7 ka represents the increasing exposure to deeper layers of terrestrial organic matter on the flooding continental shelf. In this model, the majority of the sediment flux to the GBR would have been transported during the transgression prior to 8 ka, and the $\delta^{15}N$ of this N would represent surface organic matter with a $\delta^{15}N$ similar to forested soils (6.66‰). High sediment flux caused by increased rainfall and runoff (Bostock et al., 2009; Denniston et al., 2013) would eventually transport N from deeper soil horizons with an elevated $\delta^{15}N$ to the coastal reefs. This response is consistent with measured $\delta^{15}N$ from modern corals; on the southern GBR between 1965 and 2005, the mean skeletal $\delta^{15}N$ for coral from a reef 5 km off shore (Round Top Island) was 8.15 ± 1.29‰, while coral from a nearby reef 32 km offshore (Keswick Island) had an average of 5.65 ± 2.67‰ during the same time interval, while also recording low-frequency extreme flood events with values of 12–16‰ (Marion et al., 2021). Therefore, the most likely mechanism for propagation of N to the reef would be from shelf flooding and subsequent fluvial flux, noting that an aeolian source would be unlikely during a relatively wet period (Salas-Saavedra et al., 2022). It is also possible that a shift to a higher energy wave climate occurred at ~8 ka, which may have triggered the reworking of Pleistocene sediments that were not previously disturbed by the initial flooding. A combination of these factors could have resulted in sustained low water quality and high turbidity over this time period. It is also noted that elevated $\delta^{15}N$ could be from dissolved N in the water column (i.e. released from mineralised sediments settled on the shelf), and not necessarily directly from terrestrial sediment on the reef (Brodie et al., 2012).

The idea that terrestrial N discharge led to increased coral $\delta^{15}N$ during the sea level transgression cannot explain why $\delta^{15}N$ decreases to around 7‰ after 7 ka, when sea level had stabilized. One would expect that terrestrial runoff would continue to supply N to the coastal region over this period. There are a number of explanations for this. First, OTR became increasingly isolated from terrestrial discharge as sea level rose, and therefore was more likely to be impacted by upwelling. This was accompanied by generally decreasing rainfall, river discharge, and terrestrial runoff in this period (Donders et al., 2007; Denniston et al., 2013). In addition, continental shelf flooding is associated with increased denitrification which preferentially removes N from the system and leads to greater N_2 fixation (Ren et al., 2017). This has the effect of lowering $\delta^{15}N$. An alternative explanation for increased $\delta^{15}N$ between 8 and 7 ka is that greater nutrient availability upstream of OTR resulted in the isotopic fractionation of the water column N pool during transport. In this case the instantaneous product of N assimilation (Hayes, 1983) would be enriched relative to the source. However, this is unlikely to be from the Fitzroy River, which is the major source for terrigenous material discharge to OTR and the Capricorn Group (Bostock et al., 2009). However, following the highstand most Fitzroy River sediment may have been retained inshore or deflected northward by currents away from the reefs farther offshore (Ryan et al., 2007). Hence bulk water quality may have cleaned up offshore.

Our data clearly demonstrate the capacity of coral reefs to develop and grow under conditions that would otherwise appear unfavorable (Fig. 3). OTR water quality during the Holocene between 8 and 7 ka was turbid and with high concentrations of nutrients, yet coral reef growth was substantial and active. The same holds true for modern corals in inshore environments, which can display very high percent coverage (Morgan et al., 2016) despite exposure to high turbidity and episodic nutrient discharge. Although believed to be reefs operating at their environmental thresholds, it has been shown that turbid GBR reefs have an average Holocene accretion rate of 2–7 mm/yr, similar to clear-water reefs (Browne et al., 2012). However, the comparatively low rate of vertical accretion rate at OTR between 8 and 7 ka (3.3 mm/yr) clearly suggests that conditions were less favorable compared growth at other times in the Holocene. The shift in communities also indicates conditions were not suitable for fast growing species requiring clear water. If RSL were to have continued rising and poor water quality conditions continued beyond the reef's thresholds, it is possible that these conditions could have led to reef drowning, as observed in the Last Glacial Maximum (LGM) to deglacial shelf-edge reefs (Webster et al., 2018).

5. Conclusions

We show for the first time a temporal correlation between multiple independent datasets indicating higher terrestrial input to OTR between 8 and 7 ka compared to other time periods. These include: (1) elevated $\delta^{15}N$ and Ba/Ca values, pointing to increased terrestrially-sourced nutrient levels on the reef; (2) increased terrestrial influence on early Holocene water quality evident from REE + Y measurements from both corals and microbialites on the southern GBR; and (3) reef core data indicating slower, deeper growth of more sediment and turbidity tolerant coral reef communities. These independent lines of evidence provide valuable information for understanding environmental controls on the Holocene initiation of the southern GBR and demonstrates the capacity of the GBR to grow under conditions that would typically be considered adverse.

CRediT authorship contribution statement

Kelsey L. Sanborn: Primary author; collection, integration, Formal analysis. **Jody M. Webster:** Supervision, manuscript revision and corresponding author*. **Dirk Erler:** δ15N measurements and interpretation of data, manuscript revision. **Gregory E. Webb:** Data interpretation; manuscript revision. **Marcos Salas-Saavedra:** Interpretation and correlation of REE + Y data. **Yusuke Yokoyama:** Ba/Ca measurements and interpretation of data.

Declaration of competing interest

The authors declare that they have no known competing financial interests or personal relationships that could have appeared to influence the work reported in this paper.

Data availability

Data will be made available on request.

Acknowledgements

We would like to acknowledge the following grants: ARC-Discovery (DP120101793), ANZIC legacy funding (LG_ 0319) and JSPS KAKENHI (23KK0013).

Appendix A. Supplementary data

Supplementary data to this article can be found online at https://doi.org/10.1016/j.quascirev.2024.108636.

References

Alibert, C., McCulloch, M., 1997. Sr/Ca ratios in modern Porites corals from the Great Barrier Reef as a proxy for SST: calibration of the thermometer and monitoring of ENSO. Paleoceanography 12, 345–363.
Bahadori, M., Chen, C., Lewis, S., Rashti, M.R., Cook, F., Parnell, A., Esfandbod, M., Boyd, S., 2019. A novel approach of combining isotopic and geochemical signatures to differentiate the sources of sediments and particulate nutrients from different land uses. Sci. Total Environ. 655, 129–140.
Beaman, R.J., 2010. 3DGBR: a high-resolution depth model for the Great barrier reef and coral sea, marine and tropical sciences Research facility (mtsrf) Project 2.5i. 1a Final Report, MTSRF 12.
Bostock, H., Opdyke, B., Gagan, M., Fifield, L.K., 2009. Late quaternary siliciclastic/carbonate sedimentation model for the Capricorn channel, southern Great barrier reef province, Australia. Mar. Geol. 257, 107–123.
Brodie, J., Kroon, F., Schaffelke, B., Wolanski, E., Lewis, S., Devlin, M., Bohnet, I., Bainbridge, Z., Waterhouse, J., Davis, A., 2012. Terrestrial pollutant runoff to the Great Barrier Reef: an update of issues, priorities and management responses. Mar. Pollut. Bull. 65, 81–100.
Browne, N.K., Smithers, S.G., Perry, C.T., 2012. Coral reefs of the turbid inner-shelf of the Great Barrier Reef, Australia: an environmental and geomorphic perspective on their occurrence, composition and growth. Earth Sci. Rev. 115, 1–20.
Davies, P.J., Hopley, D., 1983. Growth fabrics and growth rates of Holocene reefs in the Great Barrier Reef. BMR J. Aust. Geol. Geophys. 8, 237–251.
Davies, P.J., Kinesy, D.W., 1977. Holocene reef growth - one tree, Great barrier. Mar. Geol. 24, M1–M11.
Dechnik, B., Webster, J.M., Davies, P.J., Braga, J.-C., Reimer, P.J., 2015. Holocene "turn-on" and evolution of the southern Great barrier reef: revisiting reef cores from the Capricorn bunker group. Mar. Geol. 363, 174–190.
Denniston, R.F., Wyrwoll, K.-H., Polyak, V.J., Brown, J.R., Asmerom, Y., Wanamaker Jr, A.D., LaPointe, Z., Ellerbroek, R., Barthelmes, M., Cleary, D., 2013. A stalagmite record of Holocene Indonesian–Australian summer monsoon variability from the Australian tropics. Quat. Sci. Rev. 78, 155–168.
Donders, T.H., Haberle, S.G., Hope, G., Wagner, F., Visscher, H., 2007. Pollen evidence for the transition of the Eastern Australian climate system from the post-glacial to the present-day ENSO mode. Quat. Sci. Rev. 26, 1621–1637.
Druffel, E., 1997. Geochemistry of corals: proxies of past ocean chemistry, ocean circulation and climate. Proc. Natl. Acad. Sci. USA. 94 (16), 8354–8361.
Duprey, N., Wang, X., Kim, T., Cybulski, J., Vonhof, H., Crutzen, P., Haug, G., Sigman, D., Martínez-García, A., Baker, D., 2019. Megacity development and the demise of coastal coral communities: evidence from coral skeleton δ15N records in the Pearl River estuary. Global Change Biol. 26 (3), 1338–1353.
Erler, D.V., Farid, H.T., Glaze, T.D., Carlson-Perret, N.L., Lough, J.M., 2020. Coral skeletons reveal the history of nitrogen cycling in the coastal Great Barrier Reef. Nat. Commun. 11, 1500.
Erler, D.V., Shepherd, B.O., Linsley, B.K., Nothdurft, L.D., Hua, Q., Lough, J.M., 2019. Has nitrogen supply to coral reefs in the South Pacific Ocean changed over the past 50 thousand years? Paleoceanogr. Paleoclimatol. 34, 567–579. https://doi.org/10.1029/2019PA003587.
Erler, D.V., Wang, X.T., Sigman, D.M., Scheffers, S.R., Martínez-García, A., Haug, G.H., 2016. Nitrogen isotopic composition of organic matter from a 168 year-old coral skeleton: implications for coastal nutrient cycling in the Great Barrier Reef Lagoon. Earth Planet Sci. Lett. 434, 161–170.
Erler, D.V., Wang, X.T., Sigman, D.M., Scheffers, S.R., Shepherd, B.O., 2015. Controls on the nitrogen isotopic composition of shallow water corals across a tropical reef flat transect. Coral Reefs 34, 329–338.
Gagan, M.K., Hendy, E.J., Haberle, S.G., Hantoro, W.S., 2004. Post-glacial evolution of the indo-pacific warm pool and el nino-southern oscillation. Quat. Int. 118–119, 127–143.
Hallock, P., Schlager, W., 1986. Nutrient excess and the demise of coral reefs and carbonate platforms. Palaios 389–398.
Hayes, J.M., 1983. Practice and principles of isotopic measurements in organic geochemistry. Organic geochemistry of contemporaneous and ancient sediments 5, e5.
Hembrow, S.C., Taffs, K.H., Atahan, P., Parr, J., Zawadzki, A., Heijnis, H., 2014. Diatom community response to climate variability over the past 37,000 years in the sub-tropics of the Southern Hemisphere. Sci. Total Environ. 468, 774–784.
Hobbie, E.A., Ouimette, A.P., 2009. Controls of nitrogen isotope patterns in soil profiles. Biogeochemistry 95, 355–371.
Hughes, T.P., Baird, A.H., Bellwood, D.R., Card, M., Connolly, S.R., Folke, C., Grosberg, R., Hoegh-Guldberg, O., Jackson, J.B.C., Kleypas, J., Lough, J.M., Marshall, P., Nystrom, M., Palumbi, S.R., Pandolfi, J.M., Rosen, B., Roughgarden, J., 2003. Climate change, human impacts, and the resilience of coral reefs. Science 301, 929–933.
Jupiter, S., Roff, G., Marion, G., Henderson, M., Schrameyer, V., McCulloch, M., Hoegh-Guldberg, O., 2008. Linkages between coral assemblages and coral proxies of terrestrial exposure along a cross-shelf gradient on the southern Great Barrier Reef. Coral Reefs 27, 887–903.
Kinsey, D.W., Davies, P.J., 1979. Effects of elevated nitrogen and phosphorus on coral reef growth. Limnol. Oceanogr. 24, 935–940.
Leonard, N.D., Welsh, K.J., Clark, T.R., Feng, Y.x., Pandolfi, J.M., Zhao, J.x., 2018. New evidence for "far-field" Holocene sea level oscillations and links to global climate records. Earth Planet Sci. Lett. 487, 67–73.
Lewis, S.E., Lough, J.M., Cantin, N.E., Matson, E.G., Kinsley, L., Bainbridge, Z.T., Brodie, J.E., 2018. A critical evaluation of coral Ba/Ca, Mn/Ca and Y/Ca ratios as indicators of terrestrial input: new data from the Great Barrier Reef, Australia. Geochem. Cosmochim. Acta 237, 131–154.
Lewis, S.E., Sloss, C.R., Murray-Wallace, C.V., Woodroffe, C.D., Smithers, S.G., 2013. Post-glacial sea-level changes around the Australian margin: a review. Quat. Sci. Rev. 74, 115–138.
Macintyre, I.G., 1988. Modern coral reefs of western Atlantic: new geological perspective. AAPG (Am. Assoc. Pet. Geol.) Bull. 72, 1360–1369.
Marion, G.S., Dunbar, R.B., Mucciarone, D.A., Kremer, J.N., Lansing, J.S., Arthawiguna, A., 2005. Coral skeletal δ15N reveals isotopic traces of an agricultural revolution. Mar. Pollut. Bull. 50, 931–944.
Marion, G.S., Jupiter, S.D., Radice, V.Z., Albert, S., Hoegh-Guldberg, O., 2021. Linking isotopic signatures of nitrogen in nearshore coral skeletons with sources in catchment runoff. Mar. Pollut. Bull. 173, 113054.
Marshall, J., Davies, P.J., 1982. Internal structure and Holocene evolution of one tree reef, southern Great barrier reef. Coral Reefs 1, 21–28.
McCulloch, M., Fallon, S., Wyndham, T., Hendy, E., Lough, J., Barnes, D., 2003. Coral record of increased sediment flux to the inner Great Barrier Reef since European settlement. Nature 421, 727.
McNeil, M., Nothdurft, L., Erler, D., Hua, Q., Webster, J.M., 2021. Variations in mid-to late Holocene nitrogen supply to northern Great barrier reef halimeda macroalgal bioherms. Paleoceanogr. Paleoclimatol. 36, e2020PA003871.
Montagna, P., McCulloch, M., Taviani, M., Mazzoli, C., Vendrell, B., 2006. Phosphorus in cold-water corals as a proxy for seawater nutrient chemistry. Science 312, 1788–1791.

Morgan, K.M., Perry, C.T., Smithers, S.G., Johnson, J.A., Daniell, J.J., 2016. Evidence of extensive reef development and high coral cover in nearshore environments: implications for understanding coral adaptation in turbid settings. Sci. Rep. 6, 29616.

Okai, T., Suzuki, A., Kawahata, H., Terashima, S., Imai, N., 2002. Preparation of a new Geological Survey of Japan geochemical reference material: coral JCp-1. Geostand. Newsl. 26, 95–99.

Pandolfi, J.M., Bradbury, R.H., Sala, E., Hughes, T.P., Bjorndal, K.A., Cooke, R.G., McArdle, D., McClenachan, L., Newman, M.J.H., Paredes, G., Warner, R.R., Jackson, J.B.C., 2003. Global trajectories of the long-term decline of coral reef ecosystems. Science 301, 955–958.

Ren, H., Sigman, D.M., Martínez-García, A., Anderson, R.F., Chen, M.-T., Ravelo, A.C., Straub, M., Wong, G.T., Haug, G.H., 2017. Impact of glacial/interglacial sea level change on the ocean nitrogen cycle. In: Proceedings of the National Academy of Sciences, vol. 114, pp. E6759–E6766.

Ryan, D.A., Bostock, H.C., Brooke, B.P., Marshall, J.F., 2007. Bathymetric expression of the Fitzroy River palaeochannel, northeast Australia: response of a major river to sea-level change on a semi-rimmed, mixed siliciclastic-carbonate shelf. Sediment. Geol. 201, 196–211.

Sadler, J., Webb, G., Nothdurft, L., 2015. Structure and palaeoenvironmental implications of inter-branch coenosteum-rich skeleton in corymbose Acropora species. Coral Reefs 34, 201–213.

Sadler, J., Webb, G.E., Leonard, N.D., Nothdurft, L.D., Clark, T.R., 2016. Reef core insights into mid-Holocene water temperatures of the southern Great Barrier Reef. Paleoceanography 31, 1395–1408.

Sadler, J., Webb, G.E., Nothdurft, L.D., Dechnik, B., 2014. Geochemistry-based coral palaeoclimate studies and the potential of 'non-traditional'(non-massive Porites) corals: recent developments and future progression. Earth Sci. Rev. 139, 291–316.

Saha, N., Rodriguez-Ramirez, A., Nguyen, A.D., Clark, T.R., Zhao, J.-x., Webb, G.E., 2018a. Seasonal to decadal scale influence of environmental drivers on Ba/Ca and Y/Ca in coral aragonite from the southern Great Barrier Reef. Sci. Total Environ. 639, 1099–1109.

Saha, N., Webb, G.E., Zhao, J.-X., Leonard, N.D., Nguyen, A.D., 2018b. Influence of marine biochemical cycles on seasonal variation of Ba/Ca in the near-shore coral Cyphastrea, Rat Island, southern Great Barrier Reef. Chem. Geol. 499, 71–83.

Saha, N., Webb, G.E., Zhao, J.-X., Nguyen, A.D., Lewis, S.E., Lough, J.M., 2019. Coral-based high-resolution rare earth element proxy for terrestrial sediment discharge affecting coastal seawater quality, Great Barrier Reef. Geochem. Cosmochim. Acta 254, 173–191.

Saha, N., Webb, G.E., Zhao, J.X., 2016. Coral skeletal geochemistry as a monitor of inshore water quality. Sci. Total Environ. 566–567, 652–684.

Salas-Saavedra, M., 2019. Holocene Reef Development and Water Quality Reconstruction, Heron Reef and One Tree Reef, Southern Great Barrier Reef, School of Earth and Environmental Sciences. The University of Queensland, Brisbane.

Salas-Saavedra, M., Webb, G.E., Sanborn, K.L., Zhao, J.-x., Webster, J.M., Nothdurft, L. D., Nguyen, A., 2022. Holocene microbialite geochemistry records > 6000 years of secular influence of terrigenous flux on water quality for the southern Great Barrier Reef. Chem. Geol. 604.

Sanborn, K.L., Webster, J.M., Webb, G.E., Braga, J.C., Humblet, M., Nothdurft, L., Patterson, M.A., Dechnik, B., Warner, S., Graham, T., 2020. A new model of Holocene reef initiation and growth in response to sea-level rise on the Southern Great Barrier Reef. Sediment. Geol. 105556.

Sinclair, D.J., 2005. Non-river flood barium signals in the skeletons of corals from coastal Queensland, Australia. Earth Planet Sci. Lett. 237, 354.

Sloss, C.R., Murray-Wallace, C.V., Jones, B.G., 2007. Holocene sea-level change on the southeast coast of Australia: a review. Holocene 17, 999–1014.

Studer, A.S., Sigman, D.M., Martínez-García, A., Thöle, L.M., Michel, E., Jaccard, S.L., Lippold, J.A., Mazaud, A., Wang, X.T., Robinson, L.F., 2018. Increased nutrient supply to the Southern Ocean during the Holocene and its implications for the pre-industrial atmospheric CO 2 rise. Nat. Geosci. 11, 756.

Wang, X., Sigman, D.M., Cohen, A., Sinclair, D., Sherrell, R., Weigand, M., Erler, D.V., Ren, H., 2015. Isotopic composition of skeleton-bound organic nitrogen in reef-building symbiotic corals: a new method and proxy evaluation at Bermuda. Geochem. Cosmochim. Acta 148, 179–190.

Wang, X.T., Sigman, D.M., Cohen, A.L., Sinclair, D.J., Sherrell, R.M., Cobb, K.M., Erler, D.V., Stolarski, J., Kitahara, M.V., Ren, H., 2016. Influence of open ocean nitrogen supply on the skeletal δ15N of modern shallow-water scleractinian corals. Earth Planet Sci. Lett. 441, 125–132.

Wang, X.T., Sigman, D.M., Prokopenko, M.G., Adkins, J.F., Robinson, L.F., Hines, S.K., Chai, J., Studer, A.S., Martínez-García, A., Chen, T., 2017. Deep-sea coral evidence for lower Southern Ocean surface nitrate concentrations during the last ice age. Proc. Natl. Acad. Sci. USA 114, 3352–3357.

Waterhouse, J., Schaffelke, B., Bartley, R., Eberhard, R., Brodie, J., Star, M., Thorburn, P., Rolfe, J., Ronan, M., Taylor, B., 2017. 2017 Scientific Consensus Statement: land use impacts on the Great Barrier Reef water quality and ecosystem condition. Chapter 5: overview of key findings, management implications and knowledge gaps. pp. 1–53.

Webster, J.M., Braga, J.C., Humblet, M., Potts, D.C., Iryu, Y., Yokoyama, Y., Fujita, K., Bourillot, R., Esat, T.M., Fallon, S., 2018. Response of the Great Barrier Reef to sea-level and environmental changes over the past 30,000 years. Nat. Geosci. 11, 426.

Yoshikawa, C., Makabe, A., Shiozaki, T., Toyoda, S., Yoshida, O., Furuya, K., Yoshida, N., 2015. Nitrogen isotope ratios of nitrate and N* anomalies in the subtropical South Pacific. G-cubed 16, 1439–1448.